Sensorimotor Rhythm BCI with Simultaneous High Definition-Transcranial Direct Current Stimulation Alters Task Performance

Bryan S. Baxter[1], **Bradley J. Edelman**[1], **Nicholas Nesbitt**[1], and **Bin He**[1,2,*]

[1] Department of Biomedical Engineering, University of Minnesota

[2] Institute for Engineering in Medicine, University of Minnesota

Abstract

Background—Transcranial direct current stimulation (tDCS) has been used to alter the excitability of neurons within the cerebral cortex. Improvements in motor learning have been found in multiple studies when tDCS was applied to the motor cortex before or during task learning. The motor cortex is also active during the performance of motor imagination, a cognitive task during which a person imagines, but does not execute, a movement. Motor imagery can be used with noninvasive brain computer interfaces (BCIs) to control virtual objects in up to three dimensions, but to master control of such devices requires long training times.

Objective—To evaluate the effect of high-definition tDCS on the performance and underlying electrophysiology of motor imagery based BCI.

Methods—We utilize high-definition tDCS, to investigate the effect of stimulation on motor imagery-based BCI performance across and within sessions over multiple training days.

Results—We report a decreased time-to-hit with anodal stimulation both within and across sessions. We also found differing electrophysiological changes of the stimulated sensorimotor cortex during online BCI task performance for left vs. right trials. Cathodal stimulation led to a decrease in alpha and beta band power during task performance compared to sham stimulation for right hand imagination trials.

Conclusion—These results suggest that unilateral tDCS over the motor cortex differentially affects cortical areas based on task specific neural activation.

Keywords

Transcranial direct current stimulation; tDCS; brain-computer interface; BCI; sensorimotor rhythm; motor imagery

---

[*] Correspondence: Bin He, PhD, University of Minnesota, Department of Biomedical Engineering, 7-105 NHH, 312 Church Street SE, Minneapolis, MN 55455, USA, binhe@umn.edu.

I. Introduction

Transcranial direct current stimulation (tDCS) is a noninvasive neuromodulation approach wherein a low level of current is applied through scalp electrodes into the brain [1]. Essentially, tDCS is considered to modulate the resting membrane potential of neurons within the generated electric field. This results in an increase or decrease in excitability based on neuron location and orientation with respect to the field [2]. Initial studies characterized polarity specific differences in cortical effects utilizing transcranial magnetic stimulation (TMS) to elicit motor evoked potentials (MEPs) in the hand. Nitsche and Paulus [1] examined the effects of anodal tDCS over the motor cortex and found MEPs elicited by TMS were increased in amplitude, suggesting greater cortical excitability following the stimulation, while cathodal stimulation decreased MEP amplitude, suggesting decreased cortical excitability [1]. Other studies have since characterized the effects of electrode polarity and electrode placement using in vitro and in vivo models [2–5]. In studies with healthy humans, tDCS has been found to improve (or impair) task performance based on stimulation parameters with applications involving numerical learning [6], memory [7], and attention [8]. tDCS has exhibited both acute effects lasting an hour and longitudinal effects lasting from several days to months when examining performance measures as outcome at follow-up [1,9].

The BCI field has developed noninvasive online systems that utilize sensorimotor rhythms (SMRs) modulated by motor imagination to control virtual and physical objects with the goal of expanding this control to clinical populations [10–18]. Importantly, many people with motor neuron damage are not able to control their limbs due to loss of motor control pathways, but can still generate cortical activity corresponding to the hand or limb movement by performing motor imagery (MI) [17,19]. Motor Imagery is a cognitive task consisting of kinesthetically imagining a motor movement while not executing the movement. The electrophysiological signature of MI performance is an event related desynchronization (ERD), a decrease in power relative to baseline, in the alpha (8-13 Hz) and/or beta (13-30 Hz) bands in the hemisphere contralateral to the imagined movement, and an event related synchronization (ERS) in the ipsilateral hemisphere [20]. These alpha and beta oscillations over the motor and sensorimotor cortex are referred to as sensorimotor rhythms SMRs. However, MI-based BCI is not without its challenges including lengthy training times which increases user burden and findings indicating 20% of healthy subjects may not be able to learn to self-modulate SMRs to control BCIs with current technology [21].

The brain networks underlying motor execution overlap with those that underlie motor imagery [22] and motor learning tasks have been extensively used to evaluate the behavioral effects of tDCS. Anodal stimulation over the motor cortex has resulted in a faster learning rate for implicit [23] and explicit motor learning [24] as well as retention of a learned motor paradigm [9,25]. Using cathodal stimulation, Nitsche and colleagues and Stagg and colleagues found an opposite or no effect in using these same motor learning paradigms. As a result, these studies and others (see [26,27]) conclude that applying anodal tDCS over the motor cortex can improve behavioral motor learning across motor tasks.

The effects of tDCS on motor imagination are largely unknown due in part to inconsistent findings in the literature. Initial studies suggested increased ERD resulting from MI performance following anodal stimulation in small cohorts of both healthy [28] and stroke subjects [29]. More recently, Lapenta and colleagues combined tDCS stimulation with MI found an opposite effect; anodal stimulation decreased the ERD [30]. Combining high-definition tDCS (HD-tDCS) with EEG of MI before and after high-definition anodal tDCS found similar results, a decrease in beta band ERD in the stimulated hemisphere [31]. In addition to the effect of tDCS on motor imagery, there have been multiple studies examining MI-BCI performance with tDCS. An initial study of anodal tDCS prior to BCI performance found an increased ERD over the stimulated motor cortex during BCI performance of contralateral hand motor imagination following stimulation, but no change in performance within a single session [32]. Using trained subjects, Soekadar and colleagues found no change in performance within a session for those who received anodal stimulation compared to the sham group [33], however over multiple sessions with untrained subjects they found an increase in ERD following anodal stimulation [34]. Given the current state of this research, further work needs to be done to clarify how tDCS acutely and longitudinally affects subjects' ability to modulate their SMRs.

Recently, the electrophysiological network effects of tDCS have begun to be evaluated using simultaneous EEG and MEG [31,35]. HD-tDCS systems use more electrodes, and smaller electrodes, than the standard two electrode tDCS configuration to improve the targeting of the cortical area of interest [36,37]. These characteristics allow for online recording of the EEG during stimulation and online BCI performance [31,36]. Pharmacological and behavioral evidence suggests that tDCS application during, as compared to before or after, the learning of a new motor task results in an increased learning rate and increased performance.

With these technical developments, our aim is to better understand stimulation timing and task performance on MI-based BCI ability and the underlying electrophysiology by combining EEG and HD-tDCS. We utilize HD-tDCS in order to examine the effect of multiple sessions of simultaneous high-definition tDCS and SMR-BCI on subject learning of right and left hand BCI tasks within and across sessions in BCI-naïve healthy subjects. We hypothesize that simultaneous anodal tDCS over the left primary motor cortex will improve BCI performance during and after stimulation compared to sham and cathode subjects. In addition, we hypothesize that within a session, anodal and cathodal HD-tDCS will differentially alter SMR power during task performance.

II. Methods

Experimental Setup

Subjects—29 healthy subjects (14 female; 26 right handed) naïve to MI-BCI control were recruited to participate in these experiments (Age: 18-44 years; Mean: 24.1 years; SD: 5.6 years). Subjects were blinded to their group condition and were pseudo-randomized into three groups: anodal, cathodal, and sham stimulation. Subjects participated in three experimental sessions of their assigned condition. All procedures and protocols were approved by the University of Minnesota Institutional Review Board.

Hardware Setup—A 64-channel Biosemi EEG cap with active electrodes and an ActiveTwo amplifier were used to record the EEG signal at 1024 Hz (BioSemi, Amsterdam, Netherlands). A tDCS device with a high-definition (4×1) tDCS adapter was used to deliver 2 mA of current to the center electrode with four return electrodes (Soterix Medical, NY, USA). Conductive gel (Signa Gel, Cortech Solutions) was applied to reduce electrode offsets to below 30 mV for EEG electrodes and impedances under 1 kΩ for tDCS electrodes. The EEG cap was adapted to fit HD-tDCS electrodes adjacent to EEG electrodes arranged according to the international 10/20 system. The polarity of the center electrode is indicated by the subject group condition; the combined surround electrodes received the opposite current. The center electrode was placed between C3/CP3 and surround electrodes were placed between CP3/P3, C1/FC1, C5/FC5, and C3/FC3 at a radius of 3.5 cm from the center electrode (Figure 1). For anodal and cathodal conditions the stimulation consisted of a 30 second ramp up, 20 minute constant current and 30 second ramp down. For the sham condition, the device ramped up over 30 seconds and then immediately ramped down over 15 seconds. At the end of the 20 minute stimulation window, the device was ramped up and down over 45 seconds.

Experimental Procedure

Subjects were seated in a chair 90 cm from an LCD monitor where experimental stimuli were displayed. Subjects were instructed to remain still during the experimental trials. BCI2000 software was used to present experimental stimuli and record EEG data. Subjects were instructed to kinesthetically imagine opening and closing their respective hand, or a similar action such as squeezing a ball, unilaterally based on the target location. The trial structure was the same for all BCI trials and allowed for baseline rest (3 second inter-trial interval), planning (3 seconds), and online performance recordings (6 seconds maximum) (Figure 1). Trials were aborted after 6 seconds if the subject did not acquire the target (correct trial/hit) or move the cursor equivalently in the opposite direction (incorrect trial/ miss). Subjects performed four runs of 18 trials of the left/right BCI task before stimulation (Pre Stim). Following this pre-stimulation block, the tDCS system was turned on and stimulation was started. During stimulation, subjects performed 5-6 runs depending on individual resting time (During Stim). The tDCS device was then turned off and the subject immediately performed four runs of BCI trials (immediate post-stimulation/I-Post Stim) followed by a visual oddball task for 13 minutes to engage the subject in a controlled task, while allowing a rest from the BCI task. Finally, subjects performed a final four runs of the session (delayed post-stimulation/D-Post Stim). Time between sessions was at least 48 hours.

Data Collection/BCI Control—The autoregressive filter implemented in BCI2000 was used to calculate the power in the frequency band of interest using a 16th order model with a time window of 160 ms [38]. Power in the 11-13 Hz range at C3/C4, when possible, was used to control the cursor with the control signal calculated based on a linear classifier with inputs composed of the positively weighted power in C4 and the negatively weighted power in C3. A normalizer was used with the classifier to reduce any directional bias in the cursor movement due to a subject's difference in relative power between C3 and C4. After each trial, the normalizer removes the offset by subtracting the mean and scales the classifier

output to unit variance based on the weighted sum of C3 and C4 during the online period of the preceding 30 seconds. During stimulation, using C3 was not possible on all experimental days due to stimulation artifacts, and therefore one of the 9 surround electrodes was used instead of C3 to increase the signal-to-noise ratio in the controlling electrodes. The control electrode was chosen based on online visualization of the artifact and experimenter discretion. Electrodes saturated by stimulation were removed on a session by session basis and voltages were later spherically interpolated during offline processing.

Signal Processing

Raw data was high pass filtered within hardware at 1Hz and 60Hz notch filtered. Offline processing was performed with custom scripts utilizing the EEGLAB toolbox [39] in Matlab (The Mathworks, Inc., MA, USA). Data was low pass filtered at 110 Hz and the mean of each channel was removed. Electrodes were re-referenced to the common average reference and downsampled to 250 Hz. Independent Component Analysis (fast-ICA) [40] was run on concatenated data from all non-stimulation blocks. Components corresponding to eye movement, eye blink, and muscle artifact were removed. Data was then epoched into trials; those contaminated with artifacts during baseline or task performance not removed by ICA were discarded. Data from each channel were then transformed into their time-frequency representation using a 1Hz band Morlet wavelet and the power in each time window and frequency band was computed [41]. For the EEG collected during stimulation, ICA did not completely remove all stimulation artifacts in surrounding electrodes and resulted in a difference between the during-stimulation block and the pre-/post-stimulation block power that could not be solely attributed to electrophysiological responses to stimulation. Therefore we do not directly compare left hemisphere electrophysiological results between these time blocks.

Analysis

For analysis of pre-stimulation data, we removed the first run as the control signal normalizer was not yet adapted to the subject for that day. Therefore we included 54 left/right trials for Pre Stim, 90-108 trials for During Stim, 72 for I-Post Stim, and 72 for D-Post Stim.

Primary performance outcome measures include percent valid correct (PVC) and time-to-hit (TTH) the correct target. The PVC is defined as the number of trials in which the subject hit the correct target divided by the sum of hit and miss trials, with the aborted trials not included. The time-to-hit was defined for correct trials as the time elapsed from the appearance of the ball to when the ball hit the correct target.

Primary electrophysiological outcome measures include electrode baseline power, electrode online power during task performance, and the event-related power in the alpha (8-13 Hz) and beta (15-30 Hz) bands. Analysis of electrophysiological data was only performed on correct trials. We specifically examined sensorimotor electrodes C3/C4/CP3/CP4 for each of the electrophysiological measures. In addition, we calculated the pseudo-online control signal (C4 power - C3 power) during the task performance period. The trial-by-trial event-related power change, normalized to the baseline power [20,42]. The baseline was defined as

the 1 second of the inter-trial interval prior to the target appearing. The online power used was the mean power over the task window. We calculated the correlation value between the power and right vs. left hand trials as a measure of the discriminability for individual electrodes [43].

When the measure was normally distributed, we utilized a three-level hierarchical linear model (HLM) with random effects across subjects, groups, and blocks. ANOVA and t-test analyses were performed post-hoc with Bonferroni correction for multiple comparisons. When non-normally distributed, we collapsed the data along specific dimensions (session or block) and used Kruskal-Wallis tests, with Wilcoxon rank-sum tests Bonferroni corrected for post-hoc analysis. To measure longitudinal effects, we defined each block within a session as the mean of the subject values within each group for each time-point. To measure within session effects we corrected values to the pre-stimulation values for that session. Depending on the measure, this correction was either normalization to or a subtraction of the pre-stimulation value from the post-stimulation values.

III. Results

Effects of tDCS on Performance Measures

Percent valid correct (PVC) is a measure of the accuracy of performance. Using a hierarchical linear model, we found an initial difference in PVC performance between stimulation groups for right hand trials ($p = 0.002$) and left hand trials ($p = 0.019$). For right hand trials, post-hoc analysis resulted in an overall difference between anodal stimulation and cathodal stimulation groups ($p = 0.048$) and an interaction effect of session by group for anode and cathode ($p = 0.002$). For left hand trials, post-hoc analysis resulted in a significant interaction effect of session by group for anodal and cathodal stimulation groups ($p = 0.018$). Anodal subjects had higher baseline performance (Anode: 72.7%, Sham: 70.6%, Cathode: 59.2%) and had higher performance overall, therefore we baseline subtracted the pre-stimulation value of first session. With this correction there was no significant difference in PVC based on condition for either left or right hand trials (Figure 2).

The absolute time-to-hit (TTH) was not significantly different between stimulation groups in either left or right hand trials (Table 1). When normalizing the time-to-hit to each group's initial baseline value, there was a significant difference in right hand trials between the three groups ($p = 0.039$). Post hoc analysis found a difference between the anodal group and the cathodal group ($p = 0.01$); the anodal group had a significantly decreased time-to-hit for right hand trials (Figure 3). For right hand trials within a session there was a significant difference between groups at the delayed post-stimulation time block (p = 0.003); post-hoc pairwise comparison resulted in a significant difference between anodal and cathodal groups ($p = 0.003$), and anodal and sham groups ($p = 0.004$) (Figure 4). There was no significant difference for left hand trials.

Effects of tDCS on Electrophysiological Measures

We examined the event-related power in the alpha and beta bands following stimulation within sessions and across sessions and found no significant difference between stimulation

groups at C3, CP3, C4 or CP4 for either left hand or right hand imagination trials. When normalized to pre-stimulation baseline, we found a significant difference between groups in the beta band in electrode CP3 during right hand imagination trials at the delayed post-stimulation time point ($p = 0.043$) though post-hoc pairwise comparison yielded no significant differences between groups when correcting for multiple comparisons. There was a trend towards decreased ERD in the anodal and sham groups compared to the cathode. We also found a difference in the alpha band in electrode C4 at the delayed post-stimulation time point ($p = 0.048$) for right hand imagination trials, with anodal stimulation significantly greater than cathodal stimulation ($p = 0.019$). We examined trial baseline alpha power within and across sessions normalized to the pre-stimulation power between stimulation groups and found no significant difference within sessions at C3, C4, or CP4 following stimulation. When normalized to the pre-stimulation baseline power, there were within session differences between groups at CP3 at the delayed time point in the alpha band ($p = 0.023$), but no significant pairwise comparisons with post-hoc testing. There were also significant differences at CP3 in the beta band ($p = 0.036$), with significant pairwise differences between cathode and sham ($p = 0.0125$), with sham significantly higher.

There were changes in alpha power during task performance across all groups over the course of a session. In order to visualize these changes bilaterally across the motor strip, we normalized the power at each electrode to the pre-stimulation value within each session (Figure 5). We quantitatively characterized these changes at each electrode by directly comparing the values across groups at the post-stimulation time points. There were group differences in alpha and beta power within sessions in the C3 and CP3 electrodes for right hand trials (Figure 6). For electrode C3, there was a difference in alpha power between cathode and sham groups immediately following stimulation ($p = 0.0125$). At the delayed time point there was a difference between all groups in the alpha band ($p = 0.04$) and beta band ($p = 0.028$). Post-hoc analysis resulted in a significant difference between the sham and cathodal groups at the delayed time point in alpha ($p = 0.007$) and beta ($p = 0.006$). There was also a significant difference between groups over all blocks in alpha ($p = 0.036$) with a post-hoc difference between sham and cathodal groups ($p = 0.004$) and beta ($p = 0.035$) with a difference between sham and cathodal groups ($p = 0.007$). For left hand trials, there was no significant difference between the stimulation groups at any time points (immediate post-stim, p =.20; delayed post-stim, $p = 0.07$), but there was a trend for the cathodal group to have lower power than the sham and anode groups. Similar results are found in electrode CP3 for right hand trials with a significant group difference in the alpha band at the delayed post-stim time point ($p = 0.04$) with post-hoc difference between sham and cathode ($p = 0.007$). In the beta band there were significant differences between groups immediately post-stimulation ($p = 0.038$) but no significant pairwise comparisons with post-hoc testing. There were also significant differences at the delayed post-stimulation time point between groups ($p = 0.005$) with post-hoc differences between the anode and cathode group ($p = 0.011$) and the sham and cathode group ($p = 0.002$). We did not find any difference in C4/CP4 electrodes for right or left hand trials, respectively, in the alpha or beta bands immediately post-stimulation (C4 (alpha): $p = 0.34$; $p = 0.64$; (beta): $p = 0.69$, $p = 0.91$) or delayed post-stimulation (C4 (alpha): $p = 0.43$; $p = 0.65$; (beta): $p = 0.30$; $p = 0.31$).

We found a difference between stimulation groups with measures combining electrodes and trial directions. For the pseudo-control signal, we examined the change over time within a session and found that there was a significant difference immediately following stimulation between the groups for right hand trials when normalized to the pre-stimulation baseline ($p = 0.047$). Though there was no difference in post-hoc pairwise comparisons when correcting for multiple comparisons, a trend towards an increased control signal for the anode group compared to sham was present ($p = 0.025$). There were no differences for left hand trials between groups. There were no differences in discriminability between groups following stimulation for any of the examined electrodes.

IV. Discussion

We report the results of the first study, to our knowledge, of motor imagery-based BCI with simultaneous left sensorimotor HD-tDCS on behavioral and electrophysiological measures across multiple learning sessions. Stimulation alters electrophysiology and behavior during BCI performance based on task specific neural activation within and across experimental sessions.

The primary behavioral effect of anodal HD-tDCS over the left sensorimotor cortex was a reduced time to acquire right hand imagination targets both within sessions after stimulation and across three sessions on multiple days. Previous studies did not report the effect of tDCS on BCI task timing as timing was not variable [32,33]. For motor learning tasks examining the speed of performance, Nitsche et al [23] used a serial reaction time task with left M1 stimulation and right hand movement and found anodal subjects to have a decreased reaction time compared to cathodal and sham stimulation. Our results parallel this result, though in a different paradigm where timing is not the specific target of training. In addition, similar to previous studies, we found no direct effect on the accuracy for either left or right hand trials. We did not see a significant difference in accuracy across time within a session or across sessions for any group. There is significant individual variability in performance and learning and it can take some subjects many sessions to learn to control the BCI cursor with sensorimotor rhythms [44,45].

Anodal tDCS is thought to depolarize pyramidal neurons that generate the synchronous signal recorded with EEG. Two ways this may affect the sensorimotor network utilized during MI-BCI include: the depolarization leads to greater overall synchrony as more neurons are likely to fire together, or that this resting synchrony is not significantly affected by tDCS, but nonsynchronous firing, which yields the ERD, may be affected. To evaluate the support for these hypotheses, we examined baseline power changes, task based power changes, and the ERD/ERS.

We found significant differences in the mean ERD/ERS in the beta and alpha bands, respectively, at CP3 and C4 across groups following stimulation when normalized to the pre-stimulation event-related power. Previous electrophysiological studies found mixed effects on the ERD following tDCS stimulation. Initial MI work found an increase in ERD of the stimulated hemisphere (left M1) when performing MI [28,29] and MI-BCI [32] whereas others found no change in the ERD for MI, MI-BCI, or motor observation [30,33]. In our

previous work [31], we found a decrease in beta ERD in the sensorimotor cortex of the stimulated hemisphere following HD-tDCS anodal stimulation as well as a trend towards increased ERD with cathodal stimulation, which we find here as well. Our study design differed from these previous studies in multiple ways; we applied stimulation with concurrent BCI feedback during BCI learning over three training sessions, and in the context of a single session, subjects performed the BCI task before, during, directly after, and thirty minutes after stimulation. The specific timing of stimulation relative to task performance has been found to have a significant effect on the outcome of the stimulation for motor tasks; simultaneous performance and stimulation have yielded the greatest effect [27].

We found differing effects on the baseline power and online power during task performance. There were few significant differences post-stimulation in the baseline period of the trials, which would suggest that tDCS is not affecting this alpha activity prior to task performance. We found a difference in alpha power between the stimulation groups during right hand task performance across blocks at electrodes C3 and CP3. This difference was composed of a decreased alpha power during right hand trials for cathodal stimulation compared to sham stimulation, where anodal and sham stimulation both increased following the stimulation block. This result suggests that cathodal stimulation reduces a subject's ability to modulate their SMR during task performance compared to sham stimulation. This also suggests there is not an overall change in alpha power following stimulation but rather a task specific effect. In addition, when calculating our pseudo-control signal, we found a difference in the control signal for right hand trials between groups with a trend for an increased control signal in the anodal group compared to the sham group. For right hand imagination we expect the left sensorimotor cortex to have decreased power relative to the right and anodal stimulation resulted in an increase in this signal compared to the sham stimulation.

There is a large degree of individual variability for both MI-BCI performance and responses to non-invasive brain stimulation [21,46–48]. We did not individually target the tDCS based on subject specific anatomy or functionality, targeting the area of maximum ERD/ERS during motor imagination. This could have resulted in inaccurate targeting of the stimulation area on the individual level, particularly with HD-tDCS which restricts the stimulated area compared to the standard two electrode tDCS configuration. Others have found subject specific targeting of non-invasive neuromodulation to be vital for treating neurological disorders [49]. For the BCI learning, we did not individualize parameters for each subject, rather we used the 11-13 Hz frequency band and fixed electrodes (C3/C4) for all subjects, though there can be variability in electrodes or frequencies bands that subjects use to control the BCI. This may have led to reduced accuracy across subjects and inhibited learning of the task over multiple sessions. Additionally, we did not use a source-analysis based filter the EEG control signal which may lead to improvements in performance by solving the inverse problem [50–52].

We may see differing effects compared to previous studies due to a host of parameters, including the stimulation time, the amplitude of stimulation, the timing of stimulation, as well as the electrode montage [53]. The variability across study design and parameters within MI and BCI performance, and across tDCS studies, in general, suggest significant avenues for future investigation to optimize stimulation for the target task. Recent computer

modeling work has suggested that use of simulation pipelines may help improve optimal stimulation [54–56]. Overall, the behavioral and electrophysiological results combined suggest that anodal tDCS is differentially affecting right and left hand motor imagination. Using noninvasive electrophysiological recordings during and after stimulation is a promising way of further understanding the effects of tDCS stimulation on brain networks, as without these recordings, we cannot understand the underlying physiological changes that result in the vast number of behavioral changes reported in the literature.

Acknowledgement

References

1. Nitsche MA, Paulus W. Sustained excitability elevations induced by transcranial DC motor cortex stimulation in humans. Neurology. 2001; 57:1899–901. [PubMed: 11723286]

2. Stagg C, Nitsche M. Physiological basis of transcranial direct current stimulation. Neurosci. 2011; 17:37–53. doi:10.1177/1073858410386614.

3. Dmochowski JP, Datta A, Bikson M, Su Y, Parra LC. Optimized multi-electrode stimulation increases focality and intensity at target. J Neural Eng. 2011; 8:046011. doi: 10.1088/1741-2560/8/4/046011. [PubMed: 21659696]

4. Kabakov AY, Muller P a, Pascual-Leone A, Jensen FE, Rotenberg A. Contribution of axonal orientation to pathway-dependent modulation of excitatory transmission by direct current stimulation in isolated rat hippocampus. J Neurophysiol. 2012; 107:1881–9. doi:10.1152/jn. 00715.2011. [PubMed: 22219028]

5. Johnson MD, Lim HH, Netoff TI, Connolly AT, Johnson N, Roy A, et al. Neuromodulation for brain disorders: challenges and opportunities. IEEE Trans Biomed Eng. 2013; 60:610–24. doi:10.1109/TBME.2013.2244890. [PubMed: 23380851]

6. Iuculano T, Cohen Kadosh R. The Mental Cost of Cognitive Enhancement. J Neurosci. 2013; 33:4482–6. doi:10.1523/JNEUROSCI.4927-12.2013. [PubMed: 23467363]

7. Javadi AH, Cheng P, Walsh V. Short duration transcranial direct current stimulation (tDCS) modulates verbal memory. Brain Stimul. 2012; 5:468–74. doi:10.1016/j.brs.2011.08.003. [PubMed: 21962975]

8. Pope PA, Miall RC. Task-specific facilitation of cognition by cathodal transcranial direct current stimulation of the cerebellum. Brain Stimul. 2012; 5:84–94. doi:10.1016/j.brs.2012.03.006. [PubMed: 22494832]

9. Reis J, Schambra HM, Cohen LG, Buch ER, Fritsch B, Zarahn E, et al. Noninvasive cortical stimulation enhances motor skill acquisition over multiple days through an effect on consolidation. Proc Natl Acad Sci U S A. 2009; 106:1590–5. doi:10.1073/pnas.0805413106. [PubMed: 19164589]

10. Doud AJ, Lucas JP, Pisansky MT, He B. Continuous three-dimensional control of a virtual helicopter using a motor imagery based brain-computer interface. PLoS One. 2011:6. doi:10.1371/journal.pone.0026322.

11. McFarland DJ, Sarnacki W a, Wolpaw JR. Electroencephalographic (EEG) control of three-dimensional movement. J Neural Eng. 2010; 7:036007. doi:10.1088/1741-2560/7/3/036007. [PubMed: 20460690]

12. He, B.; Gao, S.; Yuan, H.; Wolpaw, JR. Brain-Computer Interface.. In: He, B., editor. Neural Eng. Springer; 2013. p. 87-151.

13. He B, Baxter B, Edelman BJ, Cline CC, Ye WW. Noninvasive brain-computer interfaces based on sensorimotor rhythms. Proc IEEE. 2015; 103:1–19. doi:10.1109/JPROC.2015.2407272.

14. Cassady K, You A, Doud A, He B. The impact of mind-body awareness training on the early learning of a brain-computer interface. TECHNOLOGY. 2014; 02:254–60. doi:10.1142/S233954781450023X.

15. LaFleur K, Cassady K, Doud A, Shades K, Rogin E, He B. Quadcopter control in three-dimensional space using a noninvasive motor imagery-based brain-computer interface. J Neural Eng. 2013; 10:046003. doi:10.1088/1741-2560/10/4/046003. [PubMed: 23735712]

16. Yuan H, He B. Brain-Computer Interfaces Using Sensorimotor Rhythms: Current State and Future Perspectives. IEEE Trans Biomed Eng. 2014; 61:1425–35. doi:10.1109/TBME.2014.2312397. [PubMed: 24759276]

17. Wolpaw JR, McFarland DJ. Control of a two-dimensional movement signal by a noninvasive brain-computer interface in humans. Proc Natl Acad Sci U S A. 2004; 101:17849–54. doi:10.1073/pnas.0403504101. [PubMed: 15585584]

18. Edelman BJ, Johnson N, Sohrabpour A, Tong S, Thakor N, He B. Systems Neuroengineering: Understanding and Interacting with the Brain. Engineering. 2015; 1:292. doi:10.15302/J-ENG-2015078.

19. Kübler A, Nijboer F, Mellinger J, Vaughan TM, Pawelzik H, Schalk G, et al. Patients with ALS can use sensorimotor rhythms to operate a brain-computer interface. Neurology. 2005; 64:1775–7. doi:10.1212/01.WNL.0000158616.43002.6D. [PubMed: 15911809]

20. Pfurtscheller G, Silva L Da. Event-related EEG/ MEG synchronization and desynchronization: basic principles. Clin Neurophysiol. 1999; 110:1842–57. [PubMed: 10576479]

21. Blankertz B, Sannelli C, Halder S, Hammer EM, Kübler A, Müller K-R, et al. Neurophysiological predictor of SMR-based BCI performance. Neuroimage. 2010; 51:1303–9. doi:10.1016/j.neuroimage.2010.03.022. [PubMed: 20303409]

22. Lotze M, Halsband U. Motor imagery. J Physiol Paris. 2006; 99:386–95. doi:10.1016/j.jphysparis.2006.03.012. [PubMed: 16716573]

23. Nitsche MA, Schauenburg A, Lang N, Liebetanz D, Exner C, Paulus W, et al. Facilitation of implicit motor learning by weak transcranial direct current stimulation of the primary motor cortex in the human. J Cogn Neurosci. 2003; 15:619–26. doi:10.1162/089892903321662994. [PubMed: 12803972]

24. Stagg C, Jayaram G, Pastor D, Kincses ZT, Matthews PM, Johansen-Berg H. Polarity and timing-dependent effects of transcranial direct current stimulation in explicit motor learning. Neuropsychologia. 2011; 49:800–4. doi:10.1016/j.neuropsychologia.2011.02.009. [PubMed: 21335013]

25. Galea JM, Vazquez A, Pasricha N, de Xivry J-JO, Celnik P. Dissociating the roles of the cerebellum and motor cortex during adaptive learning: the motor cortex retains what the cerebellum learns. Cereb Cortex. 2011; 21:1761–70. doi:10.1093/cercor/bhq246. [PubMed: 21139077]

26. Madhavan S, Shah B. Enhancing motor skill learning with transcranial direct current stimulation - a concise review with applications to stroke. Front Psychiatry. 2012; 3:66. doi:10.3389/fpsyt.2012.00066. [PubMed: 22807918]

27. Reis J, Fritsch B. Modulation of motor performance and motor learning by transcranial direct current stimulation. Curr Opin Neurol. 2011; 24:590–6. doi:10.1097/WCO.0b013e32834c3db0. [PubMed: 21968548]

28. Matsumoto J, Fujiwara T, Takahashi O, Liu M, Kimura A, Ushiba J. Modulation of mu rhythm desynchronization during motor imagery by transcranial direct current stimulation. J Neuroeng Rehabil. 2010; 7:27. doi:10.1186/1743-0003-7-27. [PubMed: 20540721]

29. Kasashima Y, Fujiwara T, Matsushika Y, Tsuji T, Hase K, Ushiyama J, et al. Modulation of event-related desynchronization during motor imagery with transcranial direct current stimulation (tDCS) in patients with chronic hemiparetic stroke. Exp Brain Res. 2012; 221:263–8. doi:10.1007/s00221-012-3166-9. [PubMed: 22791228]

30. Lapenta OM, Minati L, Fregni F, Boggio PS. Je pense donc je fais: transcranial direct current stimulation modulates brain oscillations associated with motor imagery and movement observation. Front Hum Neurosci. 2013; 7:256. doi:10.3389/fnhum.2013.00256. [PubMed: 23761755]

31. Roy A, Baxter B, Bin He. High-Definition Transcranial Direct Current Stimulation Induces Both Acute and Persistent Changes in Broadband Cortical Synchronization: A Simultaneous tDCS&#x2013;EEG Study. IEEE Trans Biomed Eng. 2014; 61:1967–78. doi:10.1109/TBME. 2014.2311071. [PubMed: 24956615]

32. Wei P, He W, Zhou Y, Wang L. Performance of motor imagery brain-computer interface based on anodal transcranial direct current stimulation modulation. IEEE Trans Neural Syst Rehabil Eng. 2013; 21:404–15. doi:10.1109/TNSRE.2013.2249111. [PubMed: 23475381]

33. Soekadar SR, Witkowski M, Cossio EG, Birbaumer N, Cohen LG. Learned EEG-based brain self-regulation of motor-related oscillations during application of transcranial electric brain stimulation: feasibility and limitations. Front Behav Neurosci. 2014; 8:93. doi:10.3389/fnbeh. 2014.00093. [PubMed: 24672456]

34. Soekadar SR, Witkowski M, Birbaumer N, Cohen LG. Enhancing Hebbian Learning to Control Brain Oscillatory Activity. Cereb Cortex. 2015:1–7. doi:10.1093/cercor/bhu043. [PubMed: 23926113]

35. Soekadar SR, Witkowski M, Cossio EG, Birbaumer N, Robinson SE, Cohen LG. In vivo assessment of human brain oscillations during application of transcranial electric currents. Nat Commun. 2013; 4:2032. doi:10.1038/ncomms3032. [PubMed: 23787780]

36. Edwards D, Cortes M, Datta A, Minhas P, Wassermann EM, Bikson M. Physiological and modeling evidence for focal transcranial electrical brain stimulation in humans: A basis for high-definition tDCS. Neuroimage. 2013:1–10. doi:10.1016/j.neuroimage.2013.01.042.

37. Kuo H-I, Bikson M, Datta A, Minhas P, Paulus W, Kuo M-F, et al. Comparing cortical plasticity induced by conventional and high-definition 4×1 ring tDCS: a neurophysiological study. Brain Stimul. 2013; 6:644–8. doi:10.1016/j.brs.2012.09.010. [PubMed: 23149292]

38. McFarland DJ, Wolpaw JR. Sensorimotor rhythm-based brain-computer interface (BCI): model order selection for autoregressive spectral analysis. J Neural Eng. 2008; 5:155–62. doi: 10.1088/1741-2560/5/2/006. [PubMed: 18430974]

39. Delorme A, Makeig S. EEGLAB: an open source toolbox for analysis of single-trial EEG dynamics including independent component analysis. J Neurosci Methods. 2004; 134:9–21. doi: 10.1016/j.jneumeth.2003.10.009. [PubMed: 15102499]

40. Hyvarinen A. Fast and Robust Fixed-Point Algorithm for Independent Component Analysis. IEEE Trans Neur Net. 1999; 10:626–34.

41. Qin L, He B. A wavelet-based time-frequency analysis approach for classification of motor imagery for brain-computer interface applications. J Neural Eng. 2005; 2:65–72. doi: 10.1088/1741-2560/2/4/001. [PubMed: 16317229]

42. Yuan H, Doud A, Gururajan A, He B. Cortical imaging of event-related (de)synchronization during online control of brain-computer interface using minimum-norm estimates in frequency domain. IEEE Trans Neural Syst Rehabil Eng. 2008; 16:425–31. doi:10.1109/TNSRE.2008.2003384. [PubMed: 18990646]

43. Muller K-R, Krauledat M, Dornhege G, Curio G, Blankertz B. Machine learning techniques for brain-computer interfaces. Biomed Tech. 2004; 49:11–22.

44. McFarland DJ, Sarnacki WA, Vaughan TM, Wolpaw JR. Brain-computer interface (BCI) operation: Signal and noise during early training sessions. Clin Neurophysiol. 2005; 116:56–62. doi:10.1016/j.clinph.2004.07.004. [PubMed: 15589184]

45. Grosse-Wentrup M, Schölkopf B. A Review of Performance Variations in SMR-Based Brain −Computer Interfaces (BCIs). Brain-Computer Interface Res. 2013:39–51. doi: 10.1007/978-3-642-36083-1_5.

46. Bestmann S, de Berker AO, Bonaiuto J. Understanding the behavioural consequences of noninvasive brain stimulation. Trends Cogn Sci. 2015; 19:13–20. doi:10.1016/j.tics.2014.10.003. [PubMed: 25467129]

47. de Berker AO, Bikson M, Bestmann S. Predicting the behavioral impact of transcranial direct current stimulation: issues and limitations. Front Hum Neurosci. 2013; 7:613. doi:10.3389/fnhum. 2013.00613. [PubMed: 24109445]

48. Hammer EM, Halder S, Blankertz B, Sannelli C, Dickhaus T, Kleih S, et al. Psychological predictors of SMR-BCI performance. Biol Psychol. 2012; 89:80–6. doi:10.1016/j.biopsycho. 2011.09.006. [PubMed: 21964375]

49. Fox MD, Buckner RL, Liu H, Chakravarty MM, Lozano AM, Pascual-Leone A. Resting-state networks link invasive and noninvasive brain stimulation across diverse psychiatric and neurological diseases. Proc Natl Acad Sci U S A. 2014; 111:E4367–75. doi:10.1073/pnas. 1405003111. [PubMed: 25267639]

50. Qin L, Ding L, He B. Motor imagery classification by means of source analysis for brain-computer interface applications. J Neural Eng. 2004; 1:135–41. doi:10.1088/1741-2560/1/3/002. [PubMed: 15876632]

51. Kamousi B, Liu Z, He B. Classification of motor imagery tasks for brain-computer interface applications by means of two equivalent dipoles analysis. IEEE Trans Neural Syst Rehabil Eng. 2005; 13:166–71. doi:10.1109/TNSRE.2005.847386. [PubMed: 16003895]

52. Edelman BJ, Baxter B, He B. EEG Source Imaging Enhances the Decoding of Complex Right-Hand Motor Imagery Tasks. IEEE Trans Biomed Eng. 2016; 63:4–14. doi:10.1109/TBME. 2015.2467312. [PubMed: 26276986]

53. Moliadze V, Atalay D, Antal A, Paulus W. Close to threshold transcranial electrical stimulation preferentially activates inhibitory networks before switching to excitation with higher intensities. Brain Stimul. 2012; 5:505–11. doi:10.1016/j.brs.2011.11.004. [PubMed: 22445135]

54. Lee WH, Lisanby SH, Laine AF, Peterchev AV. Electric Field Model of Transcranial Electric Stimulation in Nonhuman Primates: Correspondence to Individual Motor Threshold. IEEE Transactions on Biomedical Engineering. 2015; 9:2095–2105.

55. Song B, Wen P, Ahfock T, Li Y. Numeric Investigation of Brain Tumor Influence on the Current Distributions During Transcranial Direct Current Stimulation. IEEE Transactions on Biomedical Engineering. 2015; 1:176–187.

56. Noetscher GM, Janakinadh Yanamadala J, Makarov SN, Pascual-Leone A. Comparison of Cephalic and Extracephalic Montages for Transcranial Direct Current Stimulation—A Numerical Study. IEEE Transactions on Biomedical Engineering. 2014; 9:2488–2498.

Highlights

- There are differential effects of left sensorimotor cortex HD-tDCS stimulation on sensorimotor rhythm based BCI performance and electrophysiology.

- Anodal HD-tDCS decreased the time to hit correct targets during contralateral hand motor imagination.

- Cathodal HD-tDCS decreased alpha and beta power during contralateral hand motor imagination trials compared to controls.

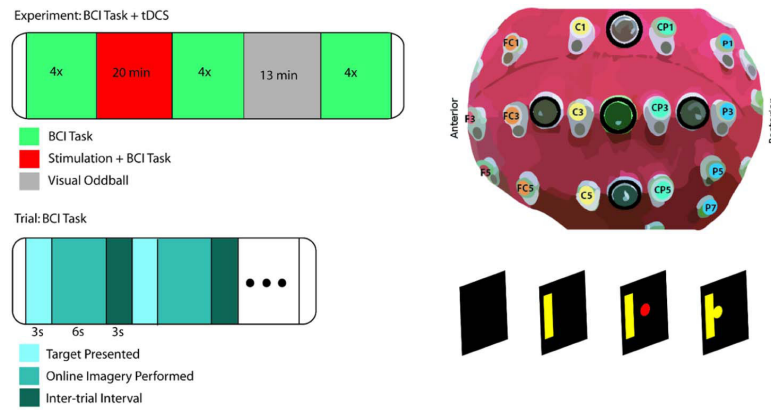- These effects should be considered when combining sensorimotor tDCS with tasks involving the motor cortex.

Figure 1.
Task design and experimental setup. Experimental session: the subject performs 4 runs of 18 trials before stimulation, undergoes 20 minutes of stimulation and BCI trials, performs 4 runs after stimulation, performs a 13 minute visual oddball experiment with right hand response, and performs 4 runs delayed after stimulation (upper left). Setup of HD-tDCS electrodes (black circles) embedded within the 64 channel EEG cap (upper right). Single trial sequence of events: after the target is presented for 3 seconds, a red ball appears on the screen and moves based on the SMR control signal for a maximum of 6 seconds, and followed by a 3 second inter-trial interval (lower panel).
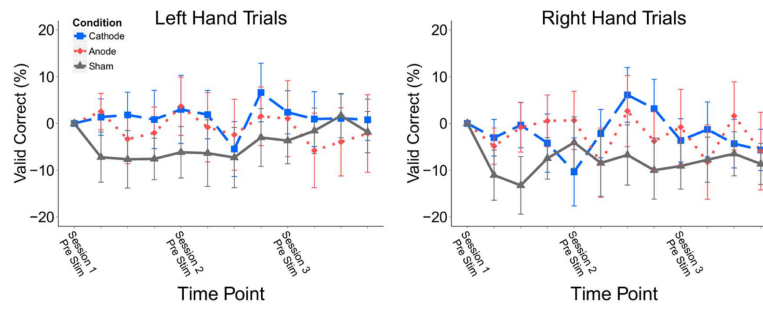
Figure 2.
Percent valid correct across time for left and right hand trials with the baseline from each individual first session pre-stimulation block subtracted from the values at later time points. Time points represent session-block PVC values, starting at Pre-stim Session One and ending at Delayed Post-stim Session Three. Group PVC did not significantly change over the three sessions. Values: Mean +/− S.E.
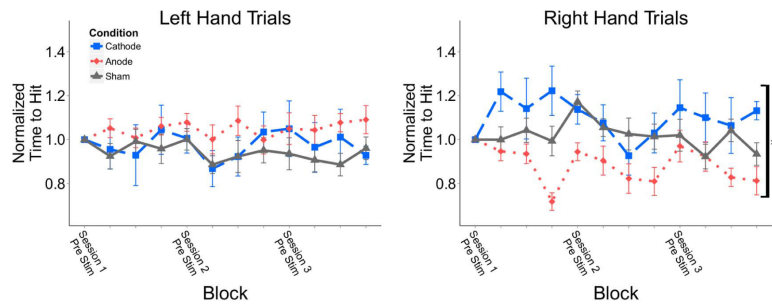
Figure 3.
Time to successfully hit right and left hand targets within experimental sessions normalized to subject initial baseline prior to stimulation. Time points represent session-block PVC values, starting at Pre-stim Session One and ending at Delayed Post-stim Session Three. The anodal group displayed a reduced time-to-hit for right hand trials compared to the cathodal group. There was no difference for left hand trials. Values: Mean +/− S.E. *p<0.05 for Kruskal Wallis test.
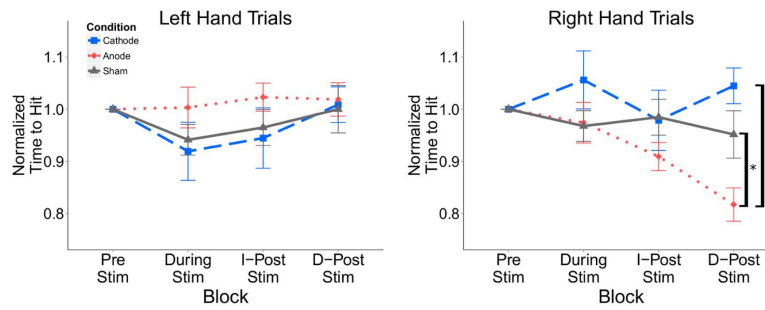
Figure 4.
Time to successfully hit right and left hand targets within experimental sessions normalized to the pre-stimulation baseline for each session. The anodal group had a reduced time-to-hit for right hand trials following stimulation at the delayed time point for right hand but not left hand trials. Values: Mean +/− S.E. *p<0.05 for Wilcoxon rank sum test.
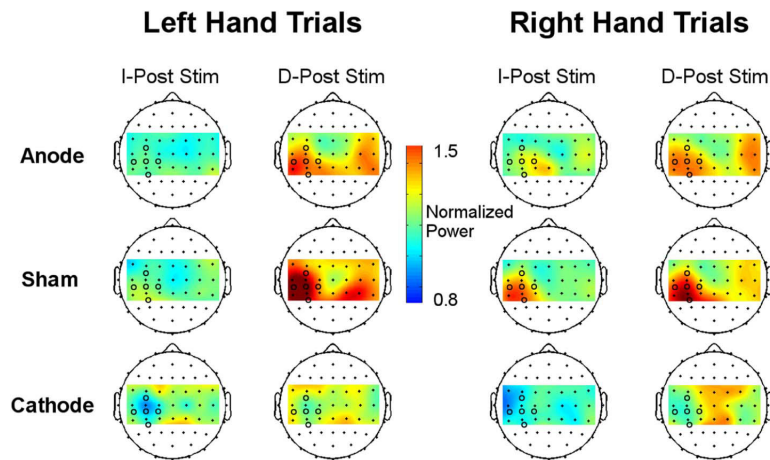
Figure 5.
Mean alpha power during task performance in the task blocks after stimulation normalized to the pre-stimulation power for left and right hand trials. For right hand trials, cathodal stimulation decreased the alpha power in the stimulated hemisphere during task performance immediately following stimulation compared to the anodal and sham groups. Colors represent power normalized to pre-stimulation baseline. Black circles represent tDCS electrodes located over the left sensorimotor cortex.
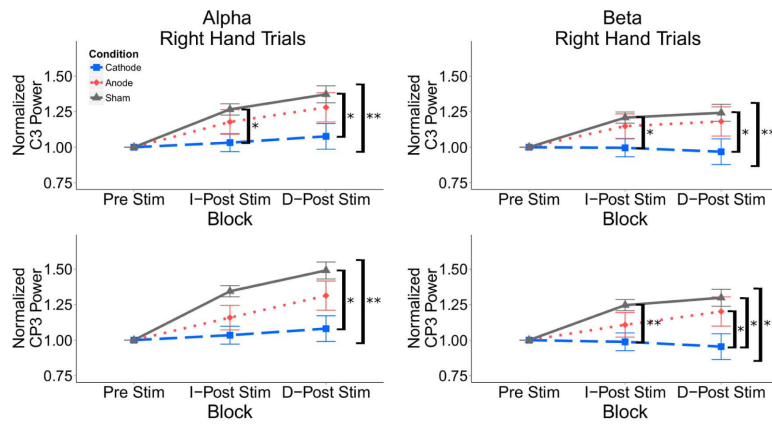
Figure 6.
Mean alpha power during task performance normalized to pre-stimulation trial power for successful right hand trials in the C3 and CP3 electrodes across the alpha (8-13Hz) and beta (15-30Hz) frequency bands. There is decreased alpha and beta power in the cathodal group compared to the sham group during right hand task performance in C3 immediately after stimulation and at the delayed post-stimulation time point and in CP3 at the delayed post-stimulation time point. There is no significant difference for left hand trials. Values: Mean +/− S.E. *p<0.0125 for Wilcoxon rank sum test. **p<0.05 for Kruskal Wallis test.

Table 1

Mean time to successfully hit right hand imagination trials across blocks. Values: Mean +/− S.E.

Right Hand Time-To-Hit (ms)	Pre Stim	I-Post Stim	D-Post Stim
Anode	3325 ± 167	2933 ± 87	2686 ± 163
Sham	3191 ± 142	3005 ± 160	2906 ± 90
Cathode	3130 ± 173	2946 ± 116	3165 ± 193